

# A FOURIER-Chebyshev COLLOCATION SPECTRAL METHOD FOR SIMULATION OF FLOW AROUND CIRCULAR CYLINDER

**Johnny J. Martínez R**

Department of Ocean Engineering, Federal University of Rio de Janeiro,  
EE-COPPE/UFRJ, CP68.508; 21945-970 Rio de Janeiro, RJ, Brazil  
Martinez@peno.coppe.ufrj.br

**Paulo T.T. Esperança**

Department of Ocean Engineering, Federal University of Rio de Janeiro,  
EE-COPPE/UFRJ, CP68.508; 21945-970 Rio de Janeiro, RJ, Brazil  
ptarso@peno.coppe.ufrj.br

**Abstract.** *Vortex-induced vibrations (VIV) of slender structural elements (marine cables, pipes and risers) are very important aspects to be considered in the design stage of many offshore structures, because the fatigue life of risers installed in deep water are often dominated by VIV effects. Despite the relatively fundamental nature of the problem, a small amount is known about the nature of the fluid-structure interaction.*

*The purpose of this paper is to develop a Fourier-Chebyshev collocation spectral method for computing unsteady two-dimensional viscous incompressible flow past a circular cylinder for moderate Reynolds numbers. The incompressible Navier-Stokes equations (INSE) are formulated in terms of the primitive variables, velocity and pressure. The incompressible Navier-Stokes equations in curvilinear coordinates are spectrally discretized and time integrated by a second-order mixed explicit/implicit time integration scheme. This scheme is a combination of the Crank-Nicolson scheme operating on the diffusive term and Adams-Bashforth scheme acting on the convective term. The projection method is used to split the solution of the INSE to the solution of two decoupled problems: the diffusion-convection equation (Burgers equation) to predict an intermediate velocity field and the Poisson equation for the pressure, it is used to correct the velocity field and satisfy the continuity equation. Finally, the numerical results obtained for the drag and lift coefficients around the circular cylinder are compared with results previously published.*

**Keywords.** *Vortex-induced vibration, Fourier-Chebyshev spectral method, Incompressible Navier-Stokes equations, Crank-Nicolson and Adams-Bashforth schemes, Projection method.*

## 1. Introduction

The main objective of this current work is to develop an efficient numerical method of solution for the problem of unsteady two-dimensional viscous incompressible flow past a circular cylinder for moderate Reynolds numbers. For this purpose, the numerical simulation of the incompressible viscous Navier-Stokes equations is based upon a Fourier-Chebyshev collocation spectral method in conjunction with the projection method. The motivation for the use of collocation spectral methods stems from their high precision, as well as their very low phase errors for the prediction of time-dependent flow regimes. A time integration of the equations system is performed with a semi-implicit second-order accurate scheme (Adams-Bashforth and Crank-Nicolson).

One major problem in solving incompressible Navier-Stokes equations comes from the coupling of the pressure with the velocity, to satisfy the incompressibility condition. Different methods were proposed to overcome this difficulty. The use of vorticity and streamfunction formulation of the equations avoids this problem. However, although its application to two-dimensional flows is common, its extension to three-dimensional problems is not straightforward. Thus, the primitive variable formulation is found to be most easily extended to 3-D flows. For this type of formulation, Chorin (1968) and Temam (1968) proposed the projection method (or fractional step method) to overcome the lack of evolution equation for the pressure in this formulation, which is known to be a source of difficulty.

At first, the paper presents the mathematical formulation of the projection method and the transformation of the incompressible Navier-Stokes equations for a generalized curvilinear coordinates system. A description of the Fourier-Chebyshev collocation spectral method is given. The numerical method, is presented including: grid generation; time and spatial discretization of the equations and associated boundary conditions. The numerical results of the simulations of flow around a circular cylinder for Reynolds numbers of 20, 40 and 60 are compared with previously published results. Finally, the conclusions of the numerical study of the problem are presented.

## 2. Mathematical formulation

Two-dimensional viscous incompressible fluid flows are governed by the Navier-Stokes equations. The dimensionless unsteady Navier-Stokes equations for incompressible flows in Cartesian coordinates may be written in primitive variables as

$$\frac{\partial V}{\partial t} + (V \cdot \nabla)V = -\nabla P + \frac{1}{\text{Re}} \nabla^2 V \quad \text{in } \Omega \quad (1)$$

$$\nabla \cdot V = 0 \quad \text{in } \Omega \quad (2)$$

where the unknowns are the vector  $V = (\mathbf{u}, \mathbf{v})^T$ , which represents the velocity of the flow, and the scalar  $P$ , which represents the pressure field. Here,  $\mathbf{Re}$  is the Reynolds number of the flow ( $\mathbf{Re} = U_\infty L_c / \nu$ ),  $U_\infty$  is the free-stream velocity,  $L_c$  represents the characteristic length and  $\nu$  the kinematic viscosity. Let  $\Omega$  be the internal computational domain with sufficiently smooth boundaries  $\partial\Omega$ . The initial condition is given as

$$V|_{t=0} = \mathbf{w}_0 \quad \text{in } \Omega. \quad (3)$$

satisfying Eq. (2), is important that this initial velocity field be divergence free otherwise the continuous problem does not possess a classical solution. The Eqs. (1) and (2) are completed with an appropriate boundary condition for the velocity field, such that:

$$V = \mathbf{w} \quad \text{on } \partial\Omega. \quad (4)$$

The Navier-Stokes equations were non-dimensionalized using the following dimensionless variables:

$$\mathbf{x}' = \frac{\mathbf{x}}{L_c}, \quad \mathbf{y}' = \frac{\mathbf{y}}{L_c}, \quad t' = \frac{t U_\infty}{L_c}, \quad P' = \frac{P}{\rho U_\infty^2}, \quad V' = \frac{V}{U_\infty}$$

A major difficulty to solve numerically the incompressible Navier-Stokes equations (INSE) comes from that the velocity  $V$  and the pressure  $P$  are coupled together by the incompressibility constraint  $\nabla \cdot V = 0$ . To overcome this difficulty, Chorin (1968) and Temam (1968), proposed the projection method (or fractional step method), which decouples the velocity and the pressure fields. The projection method has been widely used and has proven to be very efficient for this type of problem.

These classes of methods permit uncouple the velocity and the pressure in each time step by reducing the solution of the Navier-Stokes equations to the solution of two successive problems. The first step solves an intermediate velocity, which does not satisfy the incompressibility condition (the velocity field is not solenoidal), while in the second step the intermediate velocity is projected onto a divergence-free space. This last step is equivalent to the solution of a Poisson equation for pressure, which is used to correct the intermediate velocity in order to fulfill the incompressibility condition.

The projection methods are based on the observation that the left-hand side of Eq. (1) is a Hodge decomposition. Hence an equivalent projection scheme is given by

$$\frac{\partial V}{\partial t} = \wp \left[ -(\mathbf{V} \cdot \nabla) V + \frac{1}{\mathbf{Re}} \nabla^2 V \right]. \quad (5)$$

where  $\wp$  is the operator which projects a vector field onto the space of divergence-free vector fields with appropriate boundary conditions.

The projection  $\wp$  can be defined by the solution of a Poisson equation. Specifically, let  $\mathbf{W} = V + \nabla\phi$  be the Hodge decomposition of  $\mathbf{W}$ , where  $\phi$  is a scalar field and  $V$  is divergence-free velocity field that is required to satisfy  $V|_{\partial\Omega} = \mathbf{w}$ . Then to determine  $V$  from  $\mathbf{W}$  let (Brown et al. (2001))

$$V = \wp(\mathbf{W}) = \mathbf{W} - \nabla\phi. \quad (6)$$

where

$$\nabla^2 \phi = \nabla \cdot \mathbf{W} \quad \text{in } \Omega, \quad (7)$$

$$\hat{\mathbf{n}} \cdot \nabla \phi = \hat{\mathbf{n}} \cdot (\mathbf{W} - \mathbf{w}) \quad \text{on } \partial\Omega. \quad (8)$$

Following Streett & Macaraeg (1989/90), the semi-discretized version of a semi-implicit projection method can be written in two steps as follows:

a. The advection-diffusion step solves the intermediate velocity field  $\tilde{V}$  by

$$\frac{\tilde{V} - V^n}{\Delta t} = \frac{1}{\mathbf{Re}} \nabla^2 \tilde{V} - (\mathbf{V}^n \cdot \nabla) V^n \quad \text{in } \Omega, \quad (9)$$

with the intermediate boundary conditions

$$\hat{\mathbf{t}} \cdot \tilde{\mathbf{V}} = \hat{\mathbf{t}} \cdot \mathbf{V} + \hat{\mathbf{t}} \cdot \Delta t (2\nabla \mathbf{P}^n - \nabla \mathbf{P}^{n-1}) \quad \text{on } \partial\Omega, \quad (10)$$

$$\hat{\mathbf{n}} \cdot \tilde{\mathbf{V}} = \hat{\mathbf{n}} \cdot \mathbf{V} \quad \text{on } \partial\Omega. \quad (11)$$

b. The pressure correction step solves the Poisson equation for  $\mathbf{P}$  from

$$\nabla^2 \mathbf{P}^{n+1} = \frac{\nabla \cdot \tilde{\mathbf{V}}}{\Delta t} \quad \text{in } \Omega, \quad (12)$$

with the boundary condition:

$$\hat{\mathbf{n}} \cdot \nabla \mathbf{P}^{n+1} = \mathbf{0} \quad \text{on } \partial\Omega. \quad (13)$$

Then the velocities are updated with

$$\mathbf{V}^{n+1} = \tilde{\mathbf{V}} - \Delta t \nabla \mathbf{P}^{n+1} \quad \text{in } \Omega + \partial\Omega. \quad (14)$$

In summary, this step can be viewed as the projection of the velocity field onto the divergence-free space.

### 3. Generalized curvilinear coordinates

The problem under consideration in this paper is the determination of the two-dimensional motion of an unsteady incompressible flow of a viscous fluid past circular cylinder at moderate Reynolds number, see Fig. (1). The Navier-Stokes equations for an incompressible fluid of constant density  $\rho$  are used to describe the fluid motion. In order to solve this problem the Eqs. (1) and (2) are transformed into the generalized curvilinear coordinates  $(\xi, \eta)$  using the transformation Jacobian  $\mathbf{J} = x_\xi y_\eta - y_\xi x_\eta$ , then these equations may be written as:

$$\frac{\partial U^c}{\partial \xi} + \frac{\partial V^c}{\partial \eta} = \mathbf{0} \quad (15)$$

$$\mathbf{J} \frac{\partial V}{\partial \alpha} + \frac{\partial V}{\partial \xi} \mathbf{U}^c + \frac{\partial V}{\partial \eta} \mathbf{V}^c + \bar{\nabla} \mathbf{P} = \frac{\mathbf{1}}{\mathbf{Re}} \left\{ \frac{\partial}{\partial \xi} \left[ \frac{\partial V}{\partial \xi} \left( \frac{\alpha}{\mathbf{J}} \right) - \frac{\partial V}{\partial \eta} \left( \frac{\beta}{\mathbf{J}} \right) \right] + \frac{\partial}{\partial \eta} \left[ \frac{\partial V}{\partial \eta} \left( \frac{\gamma}{\mathbf{J}} \right) - \frac{\partial V}{\partial \xi} \left( \frac{\beta}{\mathbf{J}} \right) \right] \right\} \quad (16)$$

where  $U^c$  and  $V^c$  are contravariant velocities expressed as

$$\mathbf{U}^c = y_\eta \mathbf{u} - x_\eta \mathbf{v}, \quad \mathbf{V}^c = x_\xi \mathbf{v} - y_\xi \mathbf{u} \quad (17)$$

Here,  $\bar{\nabla}$  is a gradient operator on the  $(\xi, \eta)$  system defined by

$$\bar{\nabla} = \left( y_\eta \frac{\partial(\cdot)}{\partial \xi} - y_\xi \frac{\partial(\cdot)}{\partial \eta}, x_\xi \frac{\partial(\cdot)}{\partial \eta} - x_\eta \frac{\partial(\cdot)}{\partial \xi} \right) \quad (18)$$

and

$$\alpha = x_\eta^2 + y_\eta^2, \quad \beta = x_\xi x_\eta + y_\xi y_\eta, \quad \gamma = x_\xi^2 + y_\xi^2 \quad (19)$$

are the components of the metric tensor associated to the transformation.

The Reynolds number  $\mathbf{Re}$  of the flow is based on the diameter of the cylinder  $\mathbf{D}$  ( $2r_c$ ) and the free-stream velocity  $\mathbf{U}_\infty$ .

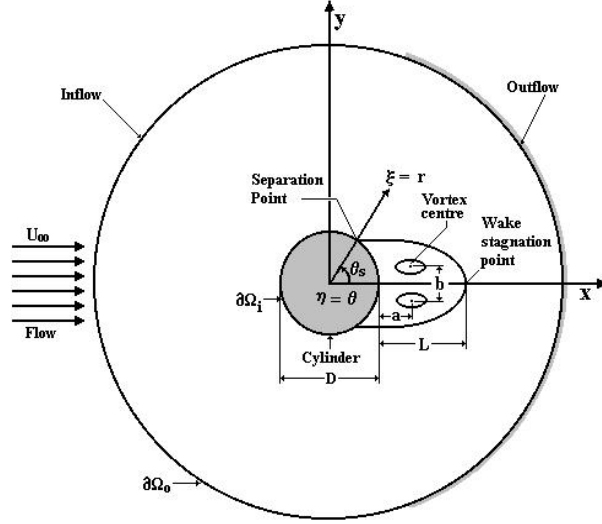


Figure 1. Flow configuration past a circular cylinder.

#### 4. Collocation spectral method

The collocation spectral method is characterized by the fact that the solution discretized is forced to satisfy the governing equations only at collocation points. So, the series expansion for a function  $\mathbf{u}(\xi)$  may be approximated as

$$\mathbf{u}_N(\xi) = \sum_{k=0}^N \hat{\mathbf{u}}_k \phi_k(\xi), \quad (20)$$

where the  $\phi_k(\xi)$  are the basis functions and the  $\hat{\mathbf{u}}_k$  are the expansion coefficients. For a Chebyshev collocation scheme, the functions  $\phi_k(\xi) = T_k(\xi) = \cos(k \cos^{-1} \xi)$  are the Chebyshev polynomials and the interpolation points are the called Chebyshev-Gauss-Lobatto points

$$\xi_i = \cos\left(\frac{\pi i}{N}\right), \quad i = 0, 1, \dots, N. \quad (21)$$

The expansion coefficients,  $\hat{\mathbf{u}}_k$  may be evaluated by the inverse relation

$$\hat{\mathbf{u}}_k = \frac{2}{N c_k} \sum_{i=0}^N \frac{\mathbf{u}_i}{c_i} \cos\left(\frac{k \pi i}{N}\right), \quad k = 0, 1, \dots, N. \quad (22)$$

where  $c_i$  and  $c_k = 1$  for  $i, k = 1, 2, \dots, N-1$  and  $c_0 = c_N = 2$ .

The derivative of  $\mathbf{u}_N(\xi)$  at the collocation points  $\xi_i$  is estimated by the analytical derivative of the Lagrange polynomials evaluating it at the collocation points  $\xi_i$ ,

$$\mathbf{u}'_N(\xi_i) = \sum_{k=0}^N \left[ \mathbf{D}_{ik}^{(1)} \right]_{\xi} \mathbf{u}_k, \quad (23)$$

where  $\left[ \mathbf{D}^{(1)} \right]_{\xi}$  is the Chebyshev collocation derivative matrix. This matrix  $\left[ \mathbf{D}^{(1)} \right]_{\xi}$  is given by (Canuto et al. (1988))

$$[D_{ik}^{(1)}]_{\xi} = \begin{cases} \frac{c_i(-1)^{i+k}}{c_k(\xi_i - \xi_k)}, & i \neq k, \\ -\frac{\xi_k}{2(1-\xi_k^2)}, & 1 \leq i = k \leq N-1, \\ \frac{2N^2+1}{6}, & i = k = 0, \\ -\frac{2N^2+1}{6}, & i = k = N. \end{cases} \quad (24)$$

The second collocation derivative matrix  $[D^{(2)}]_{\xi}$  can be computed analytically or by the following relation  $[D^{(2)}]_{\xi} = [D^{(1)}]^2$ , (Boyd (2001)). A similar procedure is carried out to estimate the Fourier collocation derivative matrix, by the analytical derivative of the trigonometric polynomials evaluating it at the Fourier collocation points  $\eta_j$ . The expressions for the first and second derivatives are expressed as (Peyret (2002) and Weideman et al.(2001)).

$$[D_{jl}^{(1)}]_{\eta} = \begin{cases} 0 & j = l, \\ \frac{1}{2}(-1)^{j+l} \cot\left[\frac{(j-l)\pi}{M}\right] & j \neq l. \end{cases} \quad (25)$$

$$[D_{jl}^{(2)}]_{\eta} = \begin{cases} -\frac{(2M^2+1)}{6} & j = l, \\ \frac{1}{2}(-1)^{j+l+1} \csc^2\left[\frac{(j-l)\pi}{M}\right] & j \neq l. \end{cases} \quad (26)$$

## 5. Numerical method

The grid used for our discretization is an O-type orthogonal grid ( $\beta = 0$ ) with cut in the wake behind the cylinder (see Fig. (2)), which is mapped onto the computational domain with the following transformation,

$$x(\xi, \eta) = r(\xi) \cos\theta(\eta), \quad y(\xi, \eta) = r(\xi) \sin\theta(\eta) \quad (27)$$

where

$$r_i(\xi) = \frac{1}{2}\xi_i \cdot (r_c - r_o) + \frac{1}{2}(r_c + r_o), \quad i = 0, 1, \dots, N \quad (28)$$

and

$$\theta_j = \eta_j = \frac{2\pi j}{M}, \quad j = 0, 1, \dots, M-1 \quad (29)$$

The collocation points along radial direction are the Chebyshev-Gauss-Lobatto points ( $\xi_i$ ) and the points in angular direction are the Fourier collocation points ( $\eta_j$ ).

The choice of this grid configuration is suited for the use of the Chebyshev collocation spectral method in the radial direction and the Fourier collocation spectral method in the angular periodic direction. The governing equations in generalized curvilinear coordinates are spatially discretized using a Fourier-Chebyshev collocation spectral method. All the dependent variables  $\mathbf{u}, \mathbf{v}, \mathbf{P}$  are expanded in double truncated series of Fourier-Chebyshev polynomials.

The temporal integration is performed with one of the most popular explicit-implicit schemes (or semi-implicit scheme) of second-order, which is a combination of second-order Adams-Bashforth and Crank-Nicolson schemes. To avoid severe stability limits, all the viscous terms in the radial direction are treated implicitly and all the advection terms and viscous terms in the angular direction are treated explicitly.

Now, the steps of the projection method (Eqs. (9), (12) and (14)) are transformed to a orthogonal curvilinear coordinate system. So, the components of the intermediate velocity field  $\tilde{\mathbf{V}}$  can be written as

$$\mathbf{J} \frac{\tilde{\mathbf{u}} - \mathbf{u}^n}{\Delta t} + \frac{\partial}{\partial \xi} (\mathbf{U}^c \mathbf{u})^n + \frac{\partial}{\partial \eta} (\mathbf{V}^c \mathbf{u})^n = \frac{\mathbf{1}}{\mathbf{Re}} \left\{ \mathbf{f}(\xi, \eta) \frac{\partial}{\partial \xi} \left[ \frac{\alpha}{\mathbf{J}} \frac{\partial \tilde{\mathbf{u}}}{\partial \xi} \right] + \frac{\partial}{\partial \eta} \left[ \frac{\gamma}{\mathbf{J}} \frac{\partial \mathbf{u}}{\partial \eta} \right] \right\} \quad (30)$$

$$\mathbf{J} \frac{\tilde{\mathbf{v}} - \mathbf{v}^n}{\Delta t} + \frac{\partial}{\partial \xi} (\mathbf{U}^c \mathbf{v})^n + \frac{\partial}{\partial \eta} (\mathbf{V}^c \mathbf{v})^n = \frac{\mathbf{1}}{\mathbf{Re}} \left\{ \mathbf{f}(\xi, \eta) \frac{\partial}{\partial \xi} \left[ \frac{\alpha}{\mathbf{J}} \frac{\partial \tilde{\mathbf{v}}}{\partial \xi} \right] + \frac{\partial}{\partial \eta} \left[ \frac{\gamma}{\mathbf{J}} \frac{\partial \mathbf{v}}{\partial \eta} \right] \right\} \quad (31)$$

The Poisson equation for pressure is given by:

$$\frac{\partial}{\partial \xi} \left[ \frac{\alpha}{\mathbf{J}} \frac{\partial \mathbf{P}^{n+1}}{\partial \xi} \right] + \frac{\partial}{\partial \eta} \left[ \frac{\gamma}{\mathbf{J}} \frac{\partial \mathbf{P}^{n+1}}{\partial \eta} \right] = \mathbf{f}(\xi, \eta) \left( \frac{\partial \tilde{\mathbf{U}}^c}{\partial \xi} + \frac{\partial \tilde{\mathbf{V}}^c}{\partial \eta} \right) \quad (32)$$

The velocity components are determined by following expressions:

$$\mathbf{u}^{n+1} = \tilde{\mathbf{u}} - \Delta t \left[ \frac{y_\eta}{\mathbf{J}} \frac{\partial \mathbf{P}^{n+1}}{\partial \xi} - \frac{y_\xi}{\mathbf{J}} \frac{\partial \mathbf{P}^{n+1}}{\partial \eta} \right] ; \mathbf{v}^{n+1} = \tilde{\mathbf{v}} - \Delta t \left[ \frac{x_\xi}{\mathbf{J}} \frac{\partial \mathbf{P}^{n+1}}{\partial \eta} - \frac{x_\eta}{\mathbf{J}} \frac{\partial \mathbf{P}^{n+1}}{\partial \xi} \right] \quad (33)$$

where the function  $\mathbf{f}(\xi, \eta)$  is a filter function that will be defined in the following section.

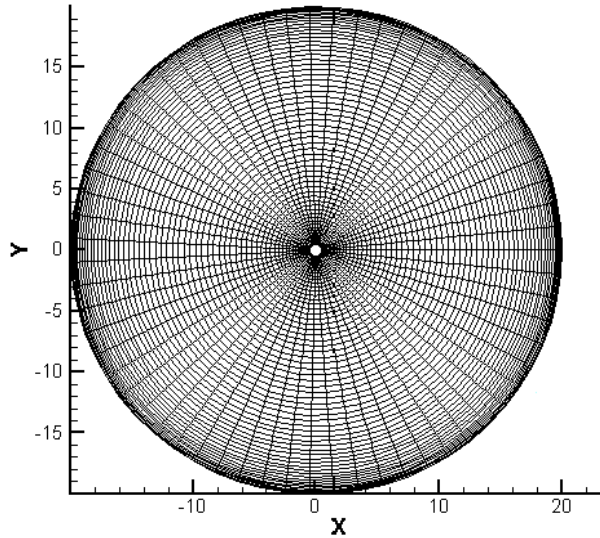


Figure 2. 2D Computational grid.

The procedure used to impose the boundary conditions on the outer computational boundary and the cylinder surface is a method devised by Mittal (1995). Due to the geometry of problem, the Fourier collocation spectral method enforces the periodicity of all variables in the azimuthal direction. Appropriate inflow and outflow boundary conditions are applied on different parts of the computational boundary. So, following Mittal (1995), a mixed boundary condition is used at the inflow boundary, which will smooth out the discontinuity in the vicinity of the inflow-outflow junction and will avoid the Gibbs phenomenon. Then, the inflow boundary for the intermediate velocity field is given by

$$\tilde{\mathbf{V}} = V_{in} - [1 - \mathbf{f}(\xi_o, \eta)] \left( \frac{\partial \tilde{\mathbf{V}}}{\partial \xi} - \frac{\partial V_{pot}}{\partial \xi} \right) \quad \text{on } \partial \Omega_{in} \quad (34)$$

where  $\xi_o$  is the extreme collocation point (outer radius),  $\partial\Omega_{in}$  is the inflow part of the outer boundary,  $V_{pot}$  is the potential velocity field and  $V_{in}$  is the Dirichlet part of the inflow boundary condition, which is defined as

$$\begin{cases} V_{in} \cdot \hat{n} = V_{pot} \cdot \hat{n} \\ V_{in} \cdot \hat{\tau} = \left[ V_{pot} + \Delta t (2\nabla P^n - \nabla P^{n-1}) \right] \cdot \hat{\tau} \end{cases} \quad (35)$$

where  $\hat{n}$  and  $\hat{\tau}$  are unit normal and tangent vectors to the boundary  $\partial\Omega_{in}$ . A buffer domain technique (Streett & Macaraeg (1989/90)) is implemented on a single domain. This technique recognizes the fact that the source of possible reflections from the outflow boundary is in the elliptic nature of the Navier-Stokes equations arising from the viscous terms and the pressure field. The idea is remove this ellipticity at the outflow boundary. Then, the first source of ellipticity; the normal viscous terms are smoothly reduced to zero at the outer boundary multiplying by a filter function  $f(\xi, \eta)$ . Similarly, the ability of the pressure field to carry signals back into the domain from the outer boundary is attenuated to zero at outflow by multiplying the source term of the pressure Poisson equation by the filter function. In the present simulations, the filter function is expressed as

$$f(\xi, \eta) = 1 - \exp \left\{ -\alpha_1 \left[ \left( \frac{r(\xi) - r_o}{r_c - r_o} \right)^{\beta_1} + \left( \frac{\eta}{\pi} \right)^{\beta_2} \right] \right\} \quad (36)$$

where  $r_c \leq r(\xi) \leq r_o$  and  $0 \leq \eta \leq \pi$ . The above function is reflected about the line of angle of attack to get its representation in the other half of the domain. The shape and smoothness of the filter function and the extent of the filtered and parabolized regions may be controlled by the parameters  $\alpha_1$ ,  $\beta_1$ , and  $\beta_2$ , (Mittal (1995)).

Outside the wake region, the diffusive effects are negligible and the flow is convective in nature. Thus, flow at the entire outflow boundary can be treated as being purely convective in the direction normal to the boundary and convective boundary conditions may be used. These boundary conditions can be obtained of the advection diffusion equations, Eqs. (31) and (32), since  $f = \mathbf{0}$  in that region.

The boundary condition for the intermediate tangential velocity component on the cylinder is given by

$$\tilde{V} \cdot \hat{\tau} = \Delta t (2\nabla P^n - \nabla P^{n-1}) \cdot \hat{\tau} \quad \text{on } \partial\Omega_i \quad (37)$$

The Eqs. (30), (31), and (32) are solved by using a complete diagonalization of the operators in both directions, (Chen et al. (2000)). The computation of eigenvalues, eigenvectors and the inversion of the corresponding matrices are done once in a preprocessing step before starting the time integration. Thus, at each time step, the solution is obtained from simple matrices products.

Finally, some characteristic coefficients of flow around a circular cylinder are defined;

$$C_L = \frac{\text{Lift force}}{0.5\rho U_\infty^2 D}, \quad C_D = \frac{\text{drag force}}{0.5\rho U_\infty^2 D}, \quad C_P = \frac{(P - P_o + \frac{1}{2}\rho U_\infty^2)}{\frac{1}{2}\rho U_\infty^2}, \quad S_t = \frac{f_s D}{U_\infty}. \quad (38)$$

$$C_{LP} = -\int_0^{2\pi} P_w \sin\theta d\theta, \quad C_{LV} = \frac{2}{\text{Re}} \int_0^{2\pi} \omega_w \cos\theta d\theta; \quad (39)$$

$$C_{DP} = -\int_0^{2\pi} P_w \cos\theta d\theta, \quad C_{DV} = -\frac{2}{\text{Re}} \int_0^{2\pi} \omega_w \sin\theta d\theta; \quad (40)$$

where  $\rho$  is the density of the fluid,  $P_o$  is the nondimensional front stagnation-point pressure,  $C_L$  is the lift coefficient,  $C_D$  is the drag coefficient and  $C_P$  is the pressure coefficient.  $S_t$  is the Strouhal number that is the nondimensional frequency of vortex shedding and  $f_s$  is the vortex shedding frequency. The subscripts  $P$  and  $V$  respectively represent the contributions of the pressure and viscous forces.  $P_w$  is the nondimensional wall pressure and  $\omega_w$  is the nondimensional wall vorticity defined as  $\omega_w = \omega r_c / U_\infty$ .

## 6. Numerical results

The numerical results were obtained by simulating the flow around a circular cylinder of a unit diameter where the outer boundary of computational domain is set at 20 cylinder diameters. The size of the O-grid generated is 83x82 and the potential flow is specified as the initial condition for all Reynolds numbers simulated.

Table (1) shows the comparison of the some results obtained for Reynolds numbers of 20 and 40 with numerical and experimental results of others authors. The results obtained by the present method are in fair agreement with the numerical results of Braza et al. (1986) and the experimental results of Coutanceau and Bouard (1977).

Table 1. Comparison of numerical and experimental results for Reynolds numbers of 20 and 40.

Author(s)	Flow quantity	Re = 20	Re = 40
Takami & Keller (1969)	<b>L/D</b>	0.935	2.325
	$\theta_s$	43.65°	53.55°
	$C_D$	2.02	1.536
Dennis & Chang (1970)	<b>L/D</b>	0.940	2.345
	$\theta_s$	43.70°	53.80°
	$C_D$	2.05	1.522
Taneda (1956) (Exp.)	<b>L/D</b>	-	2.1
	$\theta_s$	-	53.0°
Tritton (1959) (Exp.)	$C_D$	2.02	1.58
Braza et al (1986)	<b>L/D</b>	0.960	2.150
	$\theta_s$	43.60°	54.50°
	$C_D$	2.18	1.60
Coutanceau & Bouard (1977)	<b>L/D</b>	0.930	2.130
	<b>a/D ; b/D</b>	0.33 ; 0.47	0.76 ; 0.59
	$\theta_s$	44.80°	53.50°
Present method	<b>L/D</b>	0.970	2.230
	<b>a/D ; b/D</b>	0.36 ; 0.44	0.75 ; 0.60
	$\theta_s$	42.59°	52.42°
	$C_D$	2.17	1.63

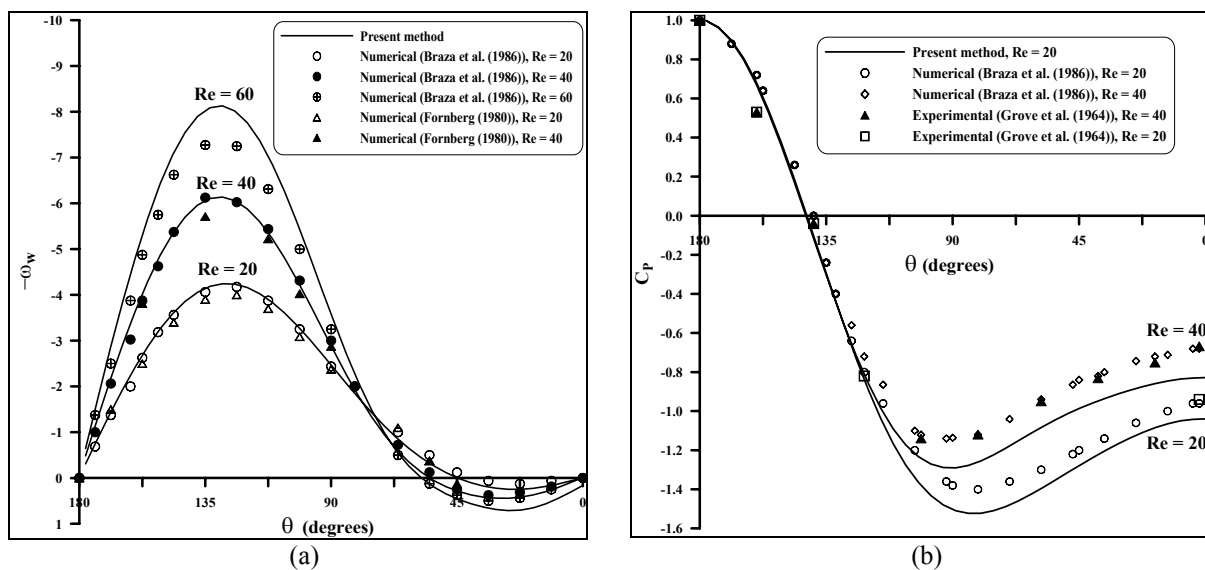


Figure 3. (a) Wall vorticity distribution for Reynolds numbers of 20, 40 and 60, (b) Pressure coefficient distribution on the cylinder for Reynolds numbers of 20 and 40.

In the Fig. (3a) the wall vorticity distribution is shown for Reynolds numbers of 20, 40 and 60 and compared with the numerical results of Braza et al. (1986) and Fornberg (1980). This comparison is found to be satisfactory for Reynolds numbers 20 and 40, but for the Reynolds number of 60, the distribution of the wall vorticity presents small discrepancies in comparison with those presented by Braza et al. (1986). Figure (3b) shows the distribution of the wall pressure coefficient compared with the numerical results of Braza et al. (1986) and the experimental results of Grove et al. (1964) for Reynolds numbers of 20 and 40. The calculation of the wall pressure coefficient by the present method agrees well with the experimental and numerical results up to  $\theta \approx 112.5^\circ$  after of this value our results one again present small discrepancies from the experimental and numerical results of the authors.

The time variation of the lift and drag coefficients for Reynolds numbers of 20, 40, 60 and 80 are shown in Figs. (4a), (4b), (4c) and (4d). For Reynolds numbers of 20 and 40, the lift coefficients are constant and equal to zero and the

drag coefficients reach constant values at very early time. The corresponding values of the drag coefficients for these Reynolds numbers are 2.17 and 1.63. For Reynolds numbers of 60 and 80, oscillations appear for both the lift and drag coefficients. These oscillations are due the alternating shedding of the vortices, which are convected and diffused away from cylinder, forming the well-known Kármán vortex street. The frequency of the oscillations of the lift coefficient in terms of the Strouhal number is found to be 0.15 for  $Re = 60$  and 0.17 for  $Re = 80$ . These results are usually bigger than the experimental Strouhal numbers values reported by Tritton (1959), (0.137 for  $Re = 60$  and 0.156 for  $Re = 80$ )

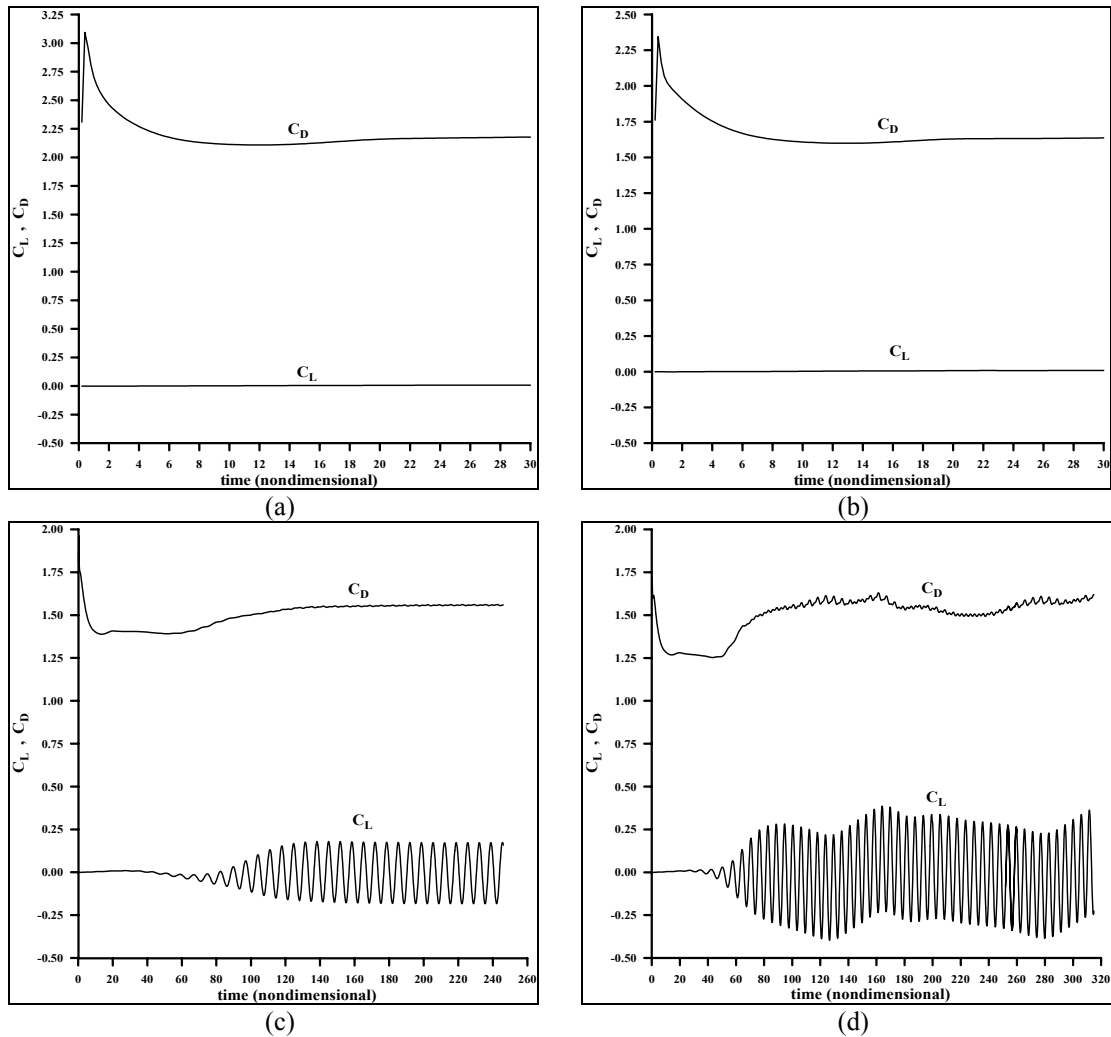


Figure 4. Time variation of the lift and drag coefficients: (a)  $Re = 20$ , (b)  $Re = 40$ , (c)  $Re = 60$ ,  $Re = 80$ .

Figures (5a), (5b) and (5c) show the streamlines around a circular cylinder for Reynolds numbers of 40, 60 and 80. In the Fig. (5a) can be noted the twin-vortices appear in the rear of cylinder at Reynolds number of 40. In the Figs. (5b) and (5c) can be observed the well-known Kármán vortex paths for numbers Reynolds of 60 and 80.

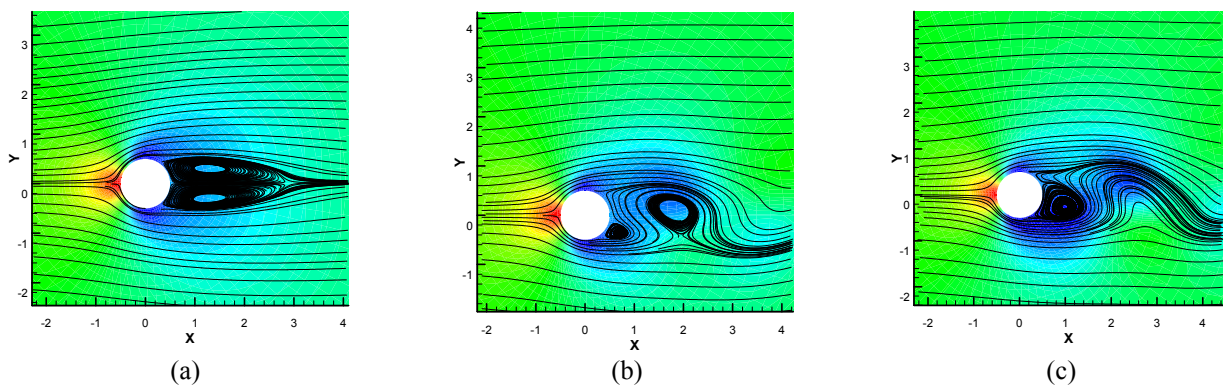


Figure 5. Streamlines around a circular cylinder: (a)  $Re = 40$ , (b)  $Re = 60$ , (c)  $Re = 80$ .

## 7. Conclusions

The projection method combined with the Fourier-Chebyshev collocation spectral method associated with a second order semi-implicit time scheme and appropriate boundary conditions, has shown to be a stable scheme and able to represent the physics of the problem of flow around a circular cylinder for moderate Reynolds numbers.

The numerical results show a very fair agreement with the numerical and experimental results previously published, especially for Reynolds numbers of 20 and 40. Small discrepancies were observed for Reynolds numbers of 60 and 80 after the starting of vortex shedding. One possible reason for these discrepancies could be the filtering process, which is applied to reduce the reflections into the domain from the outflow boundary. The determination of the optimum filter function is now under investigation.

## 8. Acknowledgement

This work was sponsored by CAPES.

The calculations were performed on computer PC-Pentium III-700 MHz of the Department of Ocean Engineering, Federal University of Rio de Janeiro, COPPE/UFRJ.

## 9. References

- Boyd, J.P., 2001, "Chebyshev and Fourier Spectral Methods", Ed. Springer-Verlag, Berlin.
- Braza, M., Chassaing, P., and Ha Minh, H., 1986, "Numerical study and physical analysis of the pressure and velocity fields in the near wake of a circular cylinder", *Journal of Fluids Mechanics*, Vol. 165, pp. 79-130.
- Brown, D.L., Cortez, R. and Minion, M.L., 2001, "Accurate projection methods for the incompressible navier-stokes equations", *Journal of Computational Physics*, Vol. 168, pp. 464-499.
- Canuto, C., Hussaini, M., Quarteroni, A. and Zang, T.A., 1988, "Spectral Methods in Fluid Dynamics", Ed. Springer-Verlag, Berlin.
- Chen, H., Su, Y. and Shizgal, B.D., 2000, "A direct spectral collocation poisson solver in polar and cylindrical coordinates", *Journal of Computational Physics*, Vol. 160, pp. 453-469.
- Chorin, A. J., 1968, "Numerical solution of the navier-stokes equations", *Mathematics of Computation*, Vol. 22, pp. 745-762.
- Coutanceau, M., and Bouard, R., 1977, "Experimental determination of the main features of the viscous flow in the wake of a circular cylinder in the uniform translation. Part 1. Steady flow", *Journal of Fluids Mechanics*, Vol. 79, pp. 231-256.
- Dennis, S.C.R., and Chang, G.Z., 1970, "Numerical solutions for steady flow past a circular cylinder at Reynolds numbers up to 100", *Journal of Fluids Mechanics*, Vol. 42, pp. 471.
- Fornberg, B., 1980, "A numerical study of steady viscous flow past a circular cylinder", *Journal of Fluids Mechanics*, Vol. 98, pp. 819-855.
- Grove, A.S., Shair, F.H., Petersen, E.E., and Acrivos A., 1964, "An experiments investigation of the steady separated flow past a circular cylinder", *Journal of Fluids Mechanics*, Vol. 19, pp. 60-85.
- Mittal, R., 1995, "Study of flow past elliptic and circular cylinders using direct numerical simulation", Ph.D. thesis, University of Illinois at Urbana, Champaign, pp. 300.
- Peyret, R., 2002, "Spectral Methods for incompressible Viscous Flow", *Applied Mathematical Sciences* 148, Springer-Verlag, Berlin.
- Streett, C.L. and Macaraeg, M.G., 1989/90, "Spectral multi-domain for large-scale fluid dynamic simulations", *Applied Numerical Mathematics*, Vol. 6, pp. 123-139.
- Takami, H., and Keller, H.B, 1969, "Steady two-dimensional viscous flow of an incompressible fluid past a circular cylinder", *The Physics of Fluids Supplement II*, Vol. 12, pp. II-51-II-56.
- Taneda, S., 1956, "Experimental investigation of the wakes behind cylinders and plates at low Reynolds numbers", *Journal of the Physical Society of Japan*, Vol. 11, pp. 302-307.
- Temam, R., 1968, "Une méthode d'approximation de la solution des équations de navier-stokes", *Bulletin of Society Mathematics of France*, Vol. 98, pp. 115-152.
- Tritton, D.J., 1959, "Experiments on the flow past a circular cylinder at low Reynolds numbers", *Journal of Fluids Mechanics*, Vol. 6, pp. 547-567.
- Weideman, J.A.C., and Reddy, S.C., 2001, "A Matlab differentiation matrix Suite", *ACM*, pp. 1-49.

## 10. Copyright Notice

The author is the only responsible for the printed material included in his paper.